Modulated Distribution of Differently Ordered Tetrahedral Chains in the Brownmillerite Structure

S. Lambert,* H. Leligny, D. Grebille, D. Pelloquin, and B. Raveau

Laboratoire CRISMAT (CNRS UMR 6508), ISMRA, 6 Bd Maréchal Juin, 14050 Caen, France

Received November 5, 2001. Revised Manuscript Received January 9, 2002

Two crystal structures $Ca_2Co_{2-x}Al_xO_5$ ($x \approx 0.75$) of brownmillerite type, have been investigated by single-crystal X-ray diffraction methods. The X-ray and electron diffraction patterns show satellite reflections, with commmensurate positions along [100]* ($a = 5.509$ Å; $b = 5.278$ Å; $c = 14.703$ Å; $\mathbf{q^*} = \alpha\mathbf{a^*}$ with $\alpha = {}^5/_8$ and ${}^2/_3$). The 4D superspace formalism was used for the refinement of these modulated structures. The average framework can be described as an alternate stacking along [001] of tetrahedral and octahedral layers formed from the metal (Co, Al) and interconnected via apical oxygen atoms. Two kinds of orientation of the tetrahedral chains, noted L (left) and R (right-hand), are evidenced, running along the [010] direction. It is shown that the L and R chains are ordered with various sequences along the modulation direction [100].

Introduction

A great deal of work has been devoted to the brownmillerite structure (Figure 1). The oxygen deficient ordered perovskite discovered by Bertaut et al.[1] for the compound $Ca_2Fe_2O_5$ consists of octahedral layers interconnected through tetrahedral chains. Bearing in mind the existence of two different coordinations for iron in this oxide, the possibility to synthesize brownmillerites $A_2BB'O_5$, characterized by an ordering of the B and B′ cations, was considered, with B and B′ adopting the octahedral and tetrahedral coordinations, respectively. This is the case of the oxides $LaACuGaO_5$,[2,3] Ca_2FeAlO_5,[4] and $A_2MnGaO_{5+\delta}$[5,6] with A = Ca, Sr, which are of potential interest for the magnetic and transport properties,[7] because of the bidimensional character of their structure.

The structure of the brownmillerite oxides $A_2BB'O_5$ is to date not really understood, despite its apparent simplicity. The best example of this complexity is shown by the oxide $Ca_2MnGaO_{5+\delta}$, whose structure is described by Abakumov et al.[5] as the result of microdomains of *Ima*2 symmetry which occur in a *Pnma* matrix, and visualized as different Ga−O chain orientations in the *Pnma* blocks. The very recent study of $Sr_2MnGaO_{5+\delta}$ [6] also shows a local ordering of the tetrahedral left (L) and right-hand (R) Ga−O chains, leading to a superstructure with a doubling of the *b* parameter of the brownmillerite. Nevertheless, the corresponding electron diffraction superlattice reflections cannot be explained in the *Ima*2 symmetry proposed for the average structure. These very interesting results suggest that the understanding of these different symmetries, and of the role of the different cations in their appearance, requires further investigations of the brownmillerite type structures.

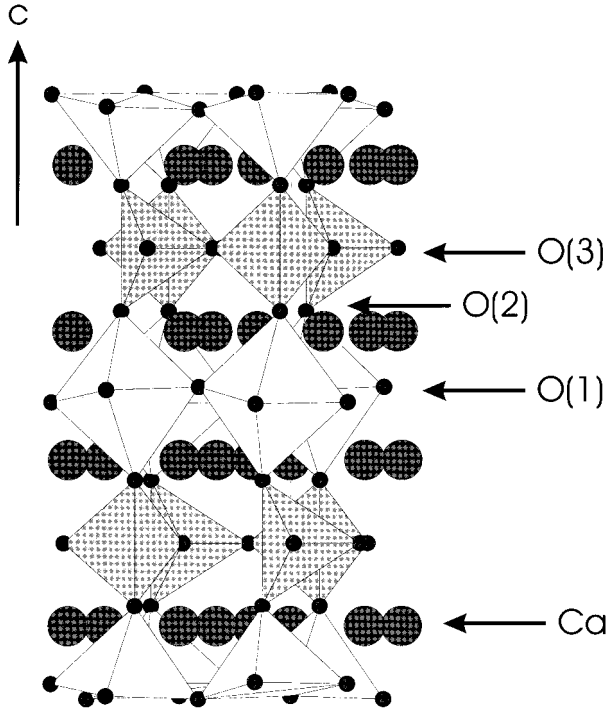

Figure 1. Stucture of brownmillerite $Ca_2M_2O_5$.

In the present study, the brownmillerites $Ca_2Co_{2-x}Al_xO_5$ have been synthesized as single crystals and a detailed single-crystal determination has been carried out using

* E-mail: lambert@ismra.fr.

(1) Bertaut, E. F.; Blum, P.; Sagnières, A. *Acta Crystallogr.* **1959**, *12*, 149−158.
(2) Kharlanov, A. L.; Antipov, E. V.; Bryntse, I.; Luzikova, A. V.; Kovbaa, L. M. *Eur. J. Solid State Inorg. Chem.* **1992**, *29*, 1041.
(3) Luzikova, A. V.; Kharlanov, A. L.; Antipov, E. V.; Muller, H. K.; Buschbaum. *Z. Anorg. Allg. Chem.* **1994**, *620*, 326.
(4) Collville, A. A.; Geller, S. *Acta Crystallogr.* **1971**, *B27*, 2311.
(5) Abakumov, A. M.; Rozova, M. G.; Pavlyuk, B. Ph.; Lobanov, M. V.; Antipov, E. V.; Lebedev, O. I.; Van Tendeloo, G.; Sheptyakov, D. V.; Balagurov, A. M.; Bouree, F. *J. Solution State Chem.* **2001**, *158*, 100−111.
(6) Abakumov, A. M.; Rozova, M. G.; Pavlyuk, B. Ph.; Lobanov, M. V.; Antipov, E. V.; Lebedev, O. I.; Van Tendeloo, G.; Ignatchik, O. L.; Ovtchenkov, E. A.; Koksharov, Yu. A.; Vasil′ev, A. N. *J. Solution State Chem.* **2001**, *160*, 353−361.
(7) Hansteen, O. H.; Fjellvag, H.; Hauback, B. C. *J. Solution State Chem.* **1998**, *141*, 411−417.

10.1021/cm011270z CCC: $22.00
Published on Web 03/23/2002

Table 1. Details of the X-ray Data Collection and of the Structure Refinement

	crystal 1	crystal 2
chemical formula	$Ca_4Co_{2.530(7)}Al_{1.470(7)}O_{10}$	$Ca_4Co_{2.475(8)}Al_{1.525(8)}O_{10}$
crystal size (mm)	0.024 × 0.144 × 0.180	0.036 × 0.245 × 0.355
crystal system	orthorhombic	orthorhombic
cell parameters (Å)		
a	5.5090(6)	5.5150(2)
b	5.2779(3)	5.2813(3)
c	14.7030(16)	14.7117(8)
V (Å^3)	427.51(7)	428.50(6)
$\mathbf{q^*} = \alpha\mathbf{a^*}$	$^5/_8$	$^2/_3$
superspace group	*Icmm*(α00)0*s*0	*Icmm*(α00)0*s*0
Z	2	2
formula weight	511.43	507.32
ρ (g·cm^{-3}); μ (cm^{-1})	3.972; 75.43	3.936; 73.66
wavelength (Å)	0.71073	0.71073
T (K)	300	300
θ_{max} (deg); (sin $\theta/\lambda)_{max}$	45; 0.995	49.92; 1.076
internal consistency factor R_{int} (after absorption correction)	2.58	1.89
extremal transmission factors		
T_{min}; T_{max}	0.3644; 0.8170	0.1846; 0.7420
no. of parameters to be refined	88	87
no. of parameters actually refined	59	58
weighting scheme	$1/\sigma^2$	$1/\sigma^2$
$\Delta\rho_{min}$ (e$^-$/Å^3)	−1.42	−1.41
$\Delta\rho_{max}$ (e$^-$/Å^3)	+1.76	1.38
no. of unique reflections (with $I \geq 3\sigma(I)$)		
hklm (the whole reflections)	1341	1971
corresponding reliability factor, R/wR (%)	2.83/3.26	2.87/4.30
*hkl*0 (main reflections)	754	1041
corresponding reliability factor, R/wR (%)	2.36/2.51	2.48/4.36
hkl±1(satellite reflections)	587	930
corresponding reliability factor, R/wR (%)	4.50/5.36	4.03/4.08

the 4D superspace formalism. We demonstrate that the different stuctures are commensurately modulated. We observed two types of orientation of the tetrahedral chains, L and R, and we show that they are ordered with various sequences along the modulation direction described by the same superspace symmetry but resulting in different 3D symmetries. On this basis, the results previously obtained for the $A_2MnGaO_{5+\delta}$ oxides are also discussed.

Synthesis

Single crystals of $Ca_2Co_{2-x}Al_xO_5$ ($0.375 < x < 0.7$) were grown during the study of the Bi−Ca−Co−Cu−O system, because of diffusion phenomena in alumina crucibles. A mixture was prepared using the oxides of calcium (CaO), bismuth (Bi_2O_3), cobalt (Co_3O_4), and copper (CuO) (Bi/Ca = 0.5; Co/Ca = 1.31; Cu/Ca = 0.83) and placed in an alumina crucible. Then, the preparation was heated to 900 °C, at 100 °C/h, and kept at this temperature for 24 h, for the decarbonation operation. It was still heated to 1100 °C, at 50 °C/h, kept at this temperature for 100 h, and then slowly cooled. Single crytals were mechanically isolated. The samples are platelet-shaped. Powder samples (of this phase) could also be synthesized, from a mixture of CaO, Co_3O_4, and Al_2O_3.

X-ray Diffraction−TEM Techniques

A preliminary study (crystal quality and symmetry) was carried out with a Weissenberg camera. The observation of satellite reflections proved the one-dimensional (1D) modulated character of all the tested samples. The electron diffraction (ED) studies were carried out using a JEOL 200CX microscope fitted with an eucentric goniometer (±60°) while the high-resolution electron microscopy (HREM) images were recorded with a TOPCON 02B operating at 200 kV and having a point resolution of 1.8 Å (Cs = 0.4 mm). Both microscopes were equipped with a KEVEX EDS analyzer. The actual cation ratio was determined from energy dispersive spectroscopy (EDS) analyses carried out on numerous crystallites. In this way, a significant Al content has been detected, leading to average Ca/Co/Al ratios close to 2:1.25:0.75, whereas neither bismuth nor copper were detected. Two crystals, with different modulations, were isolated for X-ray data collection and structure refinement. The diffracted intensities were collected on a Nonius CAD4 diffractometer, using monochromatized Mo Kα radiation (λ = 0.710 73 Å). The cell parameters were refined independently with standard techniques. Scans were performed to measure the component of the modulation wave vector along the **a*** axis. Corrections for Lorentz and polarization effects were applied to the data set. No significant intensity variation was observed during the experiment for the three chosen standard reflections. Absorption corrections, based on crystal morphology and using a Gaussian integration method, were applied to the reflection intensities with the JANA2000 program.[8] Crystal data and experimental conditions are given in Table 1.

Symmetry

A preliminary study was performed on several samples using both X-ray and electron diffraction (ED). The main experimental ED patterns are shown in Figure 2. The reconstruction of the reciprocal space leads to an orthorhombic lattice, $a_p\sqrt{2} \times a_p\sqrt{2} \times 14.7$ Å^3, with a basal plane related to the perovskite cell (a_p is the parameter

(8) Petricek, V.; Dusek, M. *The crystallographic computing system JANA2000*; Institute of Physics: Praha, Czech Republic, 2000.

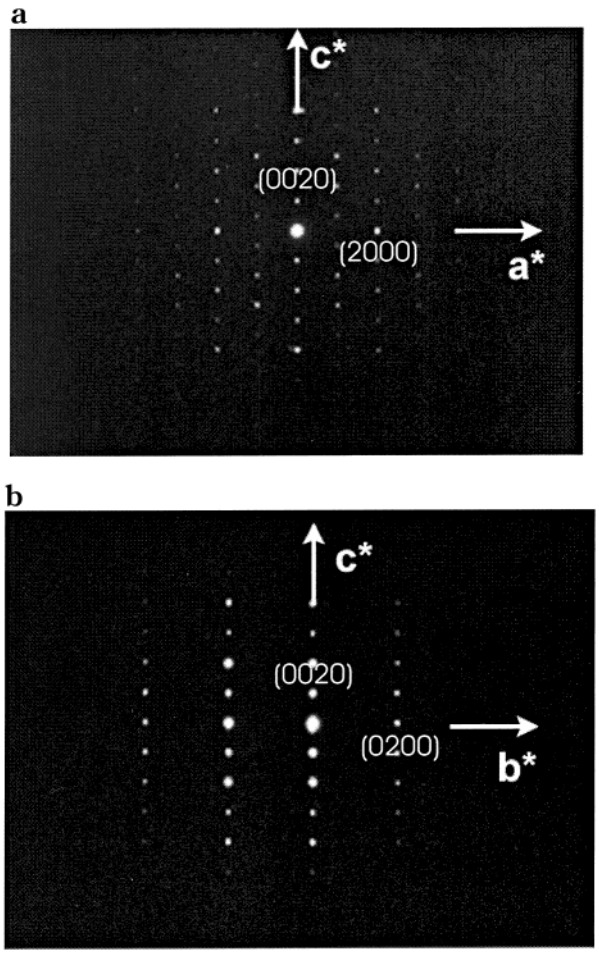

Figure 2. Experimental ED patterns recorded along the (a) [010]* and (b) [100]* directions.

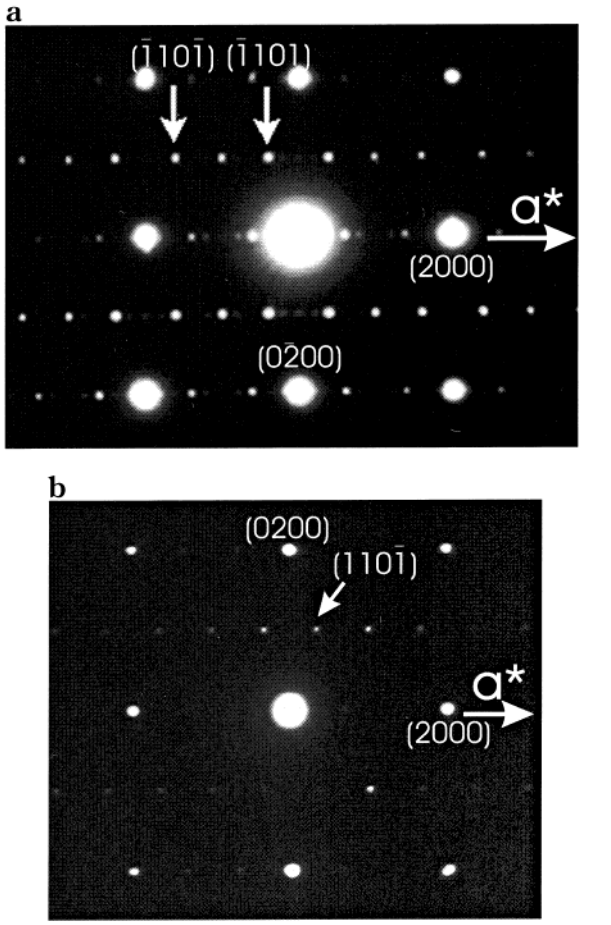

Figure 3. Experimental ED patterns recorded along [001]* showing weak extra spots (white arrows) in commensurate positions, namely $\alpha = {}^{5}/_{8}$ (a) and $\alpha = {}^{2}/_{3}$ (b).

of the cubic perovskite type structure). However, the diffraction patterns of all the studied crystals show two reflection subsets consisting of strong spots corresponding to an orthorhombic I lattice and additional spots in commensurate positions (white arrows in Figure 3), interpreted as main and satellite reflections, respectively. All the reflections conform to the *mmm* Laue symmetry. For all the crystals, the satellite reflections are defined from the modulation wave vector $\mathbf{q}^* = \alpha\mathbf{a}^*$ (Figure 3), but different rational values could be observed for the α component ($^1/_2$; $^5/_8$; $^2/_3$; $^7/_9$).

The structural study was performed on two modulated crystals exhibiting a specific α value, namely $^5/_8$ and $^2/_3$, as illustrated by both [001] electron diffraction patterns shown in Figure 3. All reflections of the latter can be indexed using the diffraction vector $\mathbf{s}^* = h\mathbf{a}^* + k\mathbf{b}^* + l\mathbf{c}^* + m\mathbf{q}^*$, where m is the satellite order. The same reflection conditions are implied for all the modulated crystals using ED or X-ray diffraction results: $hklm$, $h + k + l = 2n$; $0kl0$, $l = 2n$ ($k = 2n$); $h0lm$, $m = 2n$. These conditions are consistent with two superspace groups (SSGs): $Icmm(\alpha 00)0s0$ and $Icm2_1(\alpha 00)0s0$.[9] Since the modulation is commensurate ($\alpha = i/j$; i, j integers), the symmetry of the crystal can also be described, within the supercell $j\mathbf{a}$, $\mathbf{b}$, $\mathbf{c}$, from a 3D classical space group (SG). This 3D symmetry can be obtained[10] as a 3D symmetry restriction of the SSG symmetry by writing that the related 4D operators have to leave invariant a t section (physical space) of the 4D space. In the hypothesis of the centrosymmetrical SSG $Icmm(\alpha 00)0s0$, the results are derived and shown in Table 2. For each studied crystal, two types of particular sections are found with two possible symmetries. All the sections of the same type (modulo 1), for instance the sections $t = \nu/16$ (ν integer) in the case $\alpha = {}^5/_8$, correspond to the different possible settings of the symmetry elements in the supercell. In the *Pcam* SG case, 16 different relative positions for the 2-fold axis 2_y, the glide mirror c, and the inversion center can indeed be chosen in the supercell. In general sections t, the 3D symmetry is reduced and all the continuous t values different from the previous particular values are explained from the different possible choices of the origin along the modu-

Table 2. 3D Symmetry of the Supercell Structure Obtained for the Different *t* Sections

		t particular section		*t* general section
$\alpha = i/j$		$t = \nu/2j$	$t = (2\nu + 1)/4j$	
$\alpha = 0$		$Ic2m$	$Ic2m$	$Ic2m$
$j = 2n + 1$	$i = 2n$	$I2_1/m$	$Ic2m$	Im
	$i = 2n + 1$	$Pbnm$	$Pcnm$	$P2_1nm$
$j = 2n$		$Pcam$	$Pbam$	$P2_1am$
$\alpha = 1$		$Pbnm$	$Pcnm$	$P2_1nm$

(9) Janssen, T.; Janner, A.; Looijenga, A.; de Wolff, P. M. In *International Tables for Crystallography*; Wilson, A. J., Ed.; Kluwer Academic: Dordrecht, 1992; Vol. C797.

(10) Dam, B.; Janner, A. *Acta Crystallogr.* **1986**, *B42*, 69−77.

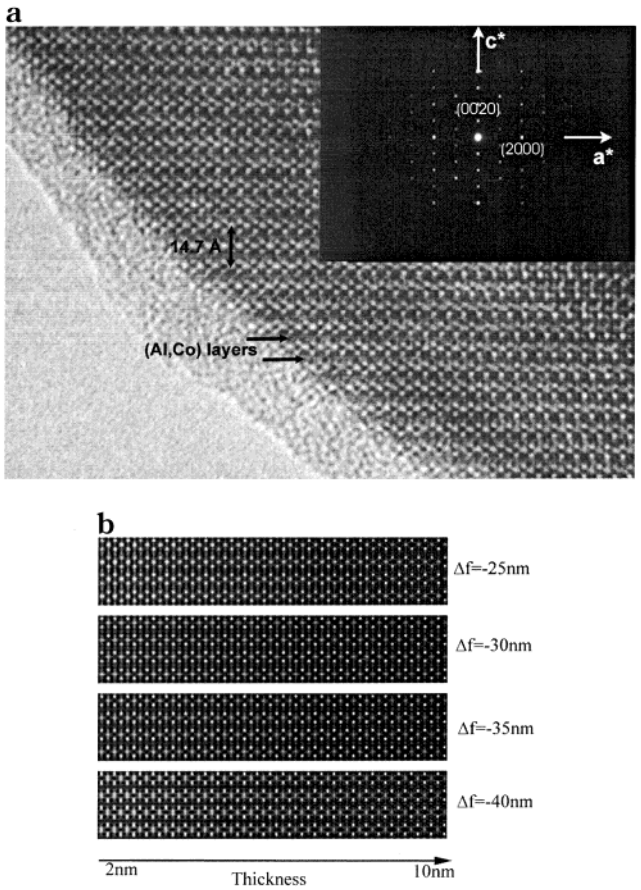

Figure 4. (a) Experimental [010] HREM image. The low electron density zones are imaged as bright dots. (b) [010] HREM simulations with various thicknesses and defocus values (Δf) calculated from a brownmillerite structural type model.

lation direction [100]. As expected, the different SGs (Table 2) deduced from the section study are subgroups of the *Icmm* SG describing the symmetry of the average structure.

Refinement

The refinements were carried out with the structure factor F values using the JANA2000 program.[8] Patterson maps calculated with the main reflections clearly show that the average structure is of the brownmillerite type[1] (Figure 1). The experimental HREM images confirm the stacking mode of this layered structure. The [010] HREM image (Figure 4), recorded with a defocus value close to −400 Å, shows a typical contrast of the Brownmillerite structure. Along the edge of the crystal, where the low electron density zones appear as bright dots, the origin of the 14.7 Å periodicity along the **c** axis can be identified. One indeed observes triple rows of bright dots alternating with single rows of gray dots along the [001] direction. These rows can be correlated to distorded [$CaCoO_3$] perovskite slabs and tetrahedral $Al_{1-y}Co_yO_4$ layers, respectively. This characteristic sequence, approximately 7.4 Å thick, is shifted by $a_p\sqrt{2}/2$ along the **a** axis, in agreement with an I-type lattice, leading to a c parameter of 14.7 Å. This structural feature is especially observed in thick zones. The $[010]_p$ images calculated from the brownmillerite type structural model (Figure 4b) for different defocus values and

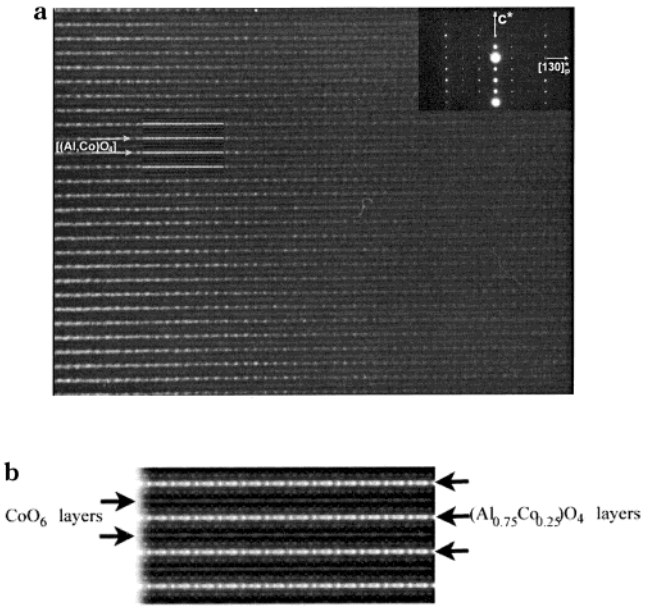

Figure 5. (a) Experimental $[3\bar{1}0]_p$ ED pattern (inset) and corresponding HREM image recorded for the modulated $\alpha = {}^2/_3$ $Ca_2Co_{1.25}Al_{0.75}O_5$ sample. The simulated $[3\bar{1}0]_p$ HREM image, calculated from the brownmillerite type subcell, is inserted. (b) The same image, calculated from supercell atomic positions.

thicknesses fit well these experimental contrasts, especially for $\Delta f = -400$ Å and a thickness close to 30 Å.

The refinement of the average structure performed assuming the *Icmm* 3D SG (reliability R factor ≈ 0.05) reveals at the level of the tetrahedral layers a splitting of the cationic (A) and oxygen (B) atomic positions on both sides of the $m_{(x,0,z)}$ mirror. This characteristic is pointed out on the $z = {}^1/_4$ section of the Fourier map (Figure 6a), where the splitted sites are labeled A_1, A_2 and B_1, B_2, respectively; the A′ and B′ sites in the figure are symmetry related to the A and B sites. The A sites are both occupied by Al and Co atoms. To determine the modulated structure of the crystal, the four-dimensional (4D) formalism[11] was used rather than the classical method requiring a study in a supercell. This method allows, from the symmetry viewpoint, a general structural description of the different crystals to be given. Indeed, a single SSG is implied for all the crystals. The modulation was assumed to be of both displacive and occupational types. The components of the displacement vector $\mathbf{U}^\mu$ of the μth atom were expanded in Fourier series

$$U_i^\mu(x_4^\mu) = \sum_n A_{i,n}^\mu \sin 2\pi\, n x_4^\mu + B_{i,n}^\mu \cos 2\pi\, n x_4^\mu$$

$$i = 1, 2, 3$$

$$x_4^\mu = \mathbf{q}^*(\mathbf{r}_0^\mu + \mathbf{p}) = \mathbf{q}^*\mathbf{r}_0^\mu + t$$

where $\mathbf{r}_0^\mu$ is the average position of the atom μ in the origin unit cell **a**, **b**, **c** and **p** is a lattice vector. Since α is rational, only some values of t are physically significant. The occupancies of the atomic sites A and B in the tetrahedral layers were modeled with crenel func-

(11) de Wolff, P. M.; Janssen, T.; Janner, A. *Acta Crystallogr.* **1981**, *A37*, 625−637.

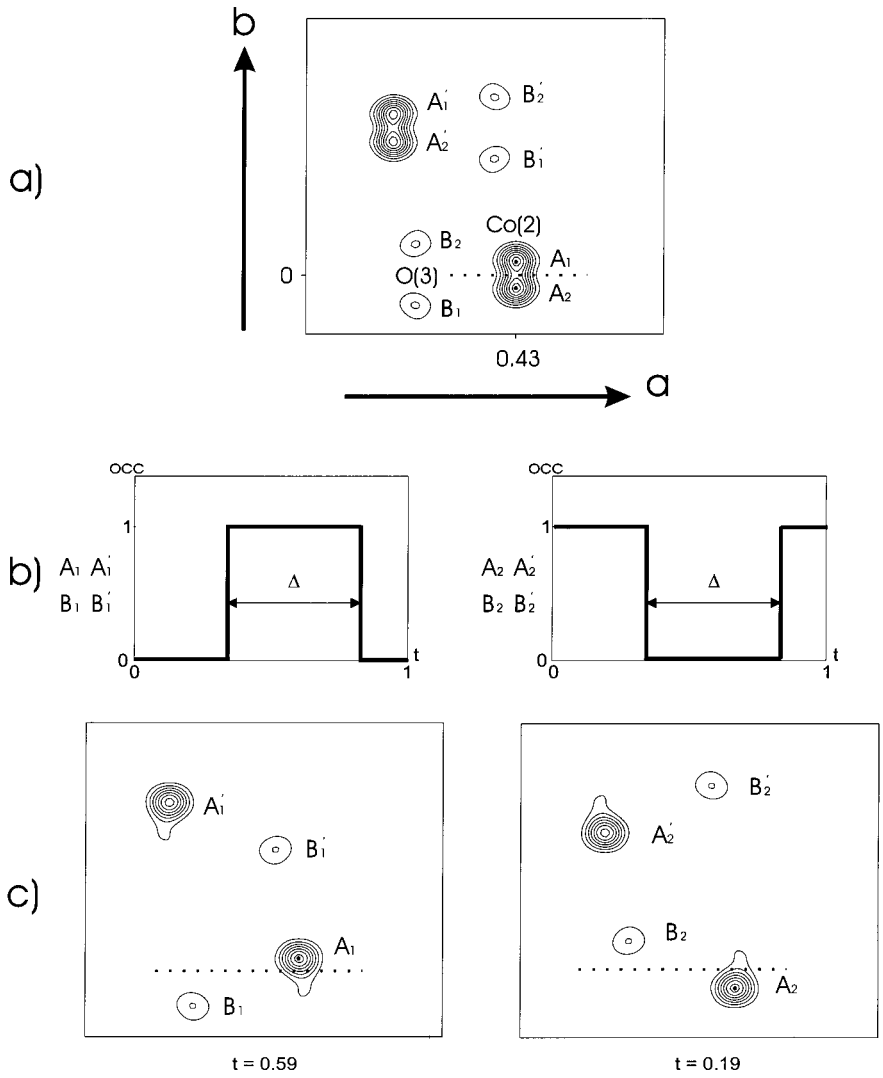

Figure 6. Two possible configurations (R and L) for the tetrahedral chains. (a) Showing of split sites for Co(2) and O(3), revealed from Fourier maps ($z = {}^1/_4$) in the average structure. (b) Occupancy modulation of the Co(2) and O(3) sites modelized from crenel functions. (c) 4D Fourier maps showing the two possible configurations of the tetrahedral chains.

tions of $\Delta = {}^1/_2$ width in x_4 assuming no vacant site (Figure 6b). Using such a function, a full occupation (occ = 1) occurs in the Δ interval and empty sites (occ = 0) are involved elsewhere. The two crenel functions for the sites A and B appeared to be in phase. This model is consistent with the 4D Fourier maps showing the section of atomic strings (Figure 6c) at different t values and will be discussed further. A displacive modulation of the A and B sites was also tried, introducing then an orthogonalization procedure.[12,13] The aluminum occupation of the two types of cobalt sites, the octahedral and the tetrahedral ones, was carefully scrutinized and refined using suited constraints, that is assuming both no vacant site and the same positions for Al and Co on the common sites. Within the octahedral layers, the Al atoms appear as distributed at random on the Co(1) sites. The introduction of a substitutional modulation does not lead to any improvement of the R factors. Within the tetrahedral layers, where a positional order is already involved for the Co(2) site A, it is more difficult to introduce such a modulation. So, only a model assuming a random partial Al occupation of the A site was considered.

To determine the actual 3D symmetry of the two studied crystals, the commensurate option was used. The refinement of the parameters was carried out considering the two types of particular sections (Table 2). For the first crystal ($\alpha = {}^5/_8$), better R factors were obtained using the *Pcam* SG rather than the *Pbam* SG. Concerning the second crystal ($\alpha = {}^2/_3$), the actual symmetry is *Ic*2*m*. Indeed, the symmetry $I2_1/m$ leads to higher R factors for the satellite reflections and implies disorder in some unit cells (at the tetrahedral chain level). Anisotropic displacement parameters (ADPs)[14] were considered for all the atoms including the oxygen atoms. The modulation of these ADPs assumed to be harmonic improved significantly the reliability R factors.

A refinement of second-order Fourier terms for the displacive modulation was attempted, using, besides the

(12) Petricek, V.; van der Lee, A.; Evain, M. *Acta Crystallogr.* **1995**, *A51*, 529−535.
(13) Boucher, F.; Evain, M.; Petricek, V. *Acta Crystallogr.* **1996**, *B52*, 100−109.
(14) Trueblood, K. N.; Bürgi, H. B.; Burlzlaff, H.; Dunitz, J. D.; Gramaccioli, C. M.; Schulz, H. H.; Shmueli, U.; Abrahams, S. C. *Acta Crystallogr.* **1996**, *A52*, 770−781.

Table 3. Structural Parameters for the Crystals Studied ($\alpha = {}^5/_8$ (in bold) and $\alpha = {}^2/_3$)

atom	*P*	*x*	*y*	*z*	U_{11}	U_{22}	U_{33}	U_{12}	U_{13}	U_{23}
Co(1)	**0.845(1)**	**0**	**1/2**	**0**	**0.00428(8)**	**0.00500(9)**	**0.0121(1)**	**0**[b]	**−0.00028(7)**	**0**[b]
	0.838(2)	0	1/2	0	0.00480(9)	0.0039(1)	0.0109(1)	0[b]	−0.00032(7)	0[b]
Al(1)	**0.155(1)**	**0**	**1/2**	**0**	**0.00428(8)**	**0.00500(9)**	**0.0121(1)**	**0**[b]	**−0.00028(7)**	**0**[b]
	0.162(2)	0	1/2	0	0.00480(9)	0.0039(1)	0.0109(1)	0[b]	−0.00032(7)	0[b]
Ca	**1**	**0.52508(4)**	**1/2**	**0.10896(2)**	**0.00899(8)**	**0.0120(1)**	**0.00853(9)**	**0**[a]	**0.00065(7)**	**0**[a]
	1	0.52540(5)	1/2	0.10894(2)	0.00937(5)	0.0112(1)	0.0072(1)	0[a]	0.00076(7)	0[a]
Co(2)	**0.420(2)**	**0.4356(1)**	**0.04692(8)**	**1/4**	**0.0089(2)**	**0.0058(2)**	**0.0078(2)**	**−0.0009(1)**	**0**[a]	**0**[a]
	0.399(3)	0.4349(1)	0.0460(1)	1/4	0.0095(3)	0.0060(2)	0.0058(2)	−0.0007(1)	0[a]	0[a]
Al(2)	**0.580(2)**	**0.4356(1)**	**0.04692(8)**	**1/4**	**0.0089(2)**	**0.0058(2)**	**0.0078(2)**	**−0.0009(1)**	**0**[a]	**0**[a]
	0.601(3)	0.4349(1)	0.0460(1)	1/4	0.0095(3)	0.0060(2)	0.0058(2)	−0.0007(1)	0[a]	0[a]
O(1)	**1**	**1/4**	**1/4**	**0.01234(7)**	**0.0100(3)**	**0.0093(3)**	**0.0159(4)**	**0.0014(3)**	**0**[a]	**0**[a]
	1	1/4	1/4	0.01233(9)	0.0116(3)	0.0071(4)	0.0129(4)	0.0010(3)	0[a]	0[a]
O(2)	**1**	**−0.0639(2)**	**1/2**	**0.14290(8)**	**0.0125(3)**	**0.0194(5)**	**0.0166(5)**	**0**[a]	**−0.0043(3)**	**0**[a]
	1	−0.0644(2)	1/2	0.1429(1)	0.0128(4)	0.0189(6)	0.0166(6)	0[a]	−0.0044(4)	0[a]
O(3)	**1**	**0.1299(3)**	**0.1041(3)**	**1/4**	**0.0100(5)**	**0.0118(6)**	**0.0131(9)**	**0.0032(4)**	**0**[a]	**0**[a]
	1	0.1301(3)	0.1055(3)	1/4	0.0124(7)	0.0118(7)	0.0109(9)	0.0035(5)	0[a]	0[a]

[a] Fixed by symmetry. [b] Fixed because not significant within their standard deviations. Only Co(2) and O(3) atoms are characterized by a crenel occupation modulation function of width $\Delta = 1/2$.

Table 4. Fourier Terms of the Displacive Modulation Obtained for the Two Structures

atom	$\bar{x}_4$ center of the crenel functions	$A_{1,1}$	$A_{2,1}$	$A_{3,1}$	$B_{1,1}$	$B_{2,1}$	$B_{3,1}$
Co(1)		**0**[a]	**0**[a]	**−0.00330(7)**	**0**[a]	**0**[a]	**0**[a]
		0[a]	0[a]	−0.00278(8)	0[a]	0[a]	0[a]
Al(1)		**0**[a]	**0**[a]	**−0.00330(7)**	**0**[a]	**0**[a]	**0**[a]
		0[a]	0[a]	−0.00278(8)	0[a]	0[a]	0[a]
Ca		**0**[a]	**0**[a]	**−0.00896(8)**	**0.01275(9)**	**0**[a]	**0**[a]
		0[a]	0[a]	−0.00728(8)	0.01237(9)	0[a]	0[a]
Co(2)	**−0.1388(7)**	**−0.0010(2)**	**−0.0013(4)**	**0**[b]	**0**[b]	**0**[a]	**0**[a]
	−0.1272(6)	0[b]	0.0011(3)	0[b]	−0.0050(5)	0[a]	0[a]
Al(2)	**−0.1388(7)**	**−0.0010(2)**	**−0.0013(4)**	**0**[b]	**0**[b]	**0**[a]	**0**[a]
	−0.1272(6)	0[b]	0.0011(3)	0[b]	−0.0050(5)	0[a]	0[a]
O(1)		**−0.0012(3)**	**0**[a]	**−0.0075(3)**	**0**[a]	**0**[a]	**0.0026(1)**
		−0.0016(3)	0[a]	−0.0060(3)	0[a]	0[a]	0.0021(1)
O(2)		**0**[a]	**0**[a]	**0.0013(3)**	**0.0217(3)**	**0**[a]	**0**[a]
		0[a]	0[a]	0[b]	0.0221(4)	0[a]	0[a]
O(3)	**0.173(1)**	**0**[b]	**0.0042(4)**	**0**[b]	**0**[b]	**0**[a]	**0**[a]
	0.168(1)	0[b]	0[b]	−0.0029(7)	0[b]	0[a]	0[a]

[a] Fixed by symmetry. [b] Fixed because not significant within their standard deviations. Only Co(2) and O(3) atoms are characterized by a crenel occupation modulation function of width $\Delta = 1/2$.

first-order satellite refletions, the second-order ones, for the most part measured with weak intensity ($I < 3\sigma(I)$). Giving arbitrary high weight to these weak satellite reflections led to second-order Fourier terms of small amplitude and of little significance. As verified, these refinement results are consistent with the F_o; that is, the F_o and F_c are about of the same magnitude for these satellite reflections. So, only the first-order satellite reflections were considered to refine the harmonic displacive modulation.

The final reliability factors on *F*, *R* (global), R_0 (main reflections), and R_1 (satellite reflections) and the corresponing wR factors are given in Table 1 for the two studied crystals; the refinement results of the two crystals ($\alpha = {}^5/_8$ (bold characters) and $\alpha = {}^2/_3$) are compared in Tables 3−5.

The previous refinement results are confirmed by HREM study. Indeed, first-order satellites are clearly visible in the $[1(\alpha - 1)0]_p$ zone axis ED patterns (Figure 5a for the $\alpha = {}^2/_3$ single crystal). The corresponding experimental $[3\bar{1}0]_p$ HREM image, shown in Figure 5a, clearly evidences an inhomogeneous contrast at the level of the bright dots row. The simulated $[3\bar{1}0]_p$ HREM image, calculated from the brownmillerite type structural model for a defocus value close to −650 Å and a thickness varying from 50 to 80 Å (inset in Figure 5a), allows us to correlate this peculiar contrast to the tetrahedral $Al_{1-y}Co_yO_4$ layers. For the modulated $\alpha = {}^2/_3$ single crystals, simulated HREM images have been carried out from atomic positions refined in the supercell 16.54 × 5.28 × 14.71 Å^3, considering the 3D *Ic*2*m* symmetry. These different calculations, especially along the direction $[3\bar{1}0]_p$ ($[1\bar{1}0]$ in the supercell) as shown in Figure 5b, corroborate our experimental contrasts and confirm the refined model.

Discussion

The present study clearly shows that brownmillerite type phases with chemical formula $Ca_2Co_{2-x}Al_xO_5$ are modulated and characterized by different modulation periods. Previous works dealing with crystals of brownmillerite type structure[1−7,15−17] did not mention any modulation, but satellite reflections were observed by TEM.[5,6]

Let us describe now the characteristics of the modulation. The main consequence of the modulated scheme consists of a perfect positional ordering of cobalt, aluminum, and oxygen atoms on the splitted sites A and B, revealed in the average structure at the level of the tetrahedral layers (Figure 6a). The occupancies of the

(15) Colville, A. A. *Acta Crystallogr.* **1970**, *B26*, 1469.
(16) Kahlenberg, V.; Shaw, C. S. J. *J. Solution State Chem.* **2001**, *157*, 62−67.
(17) Lee, J. Y.; Swennca, J. S.; Steinfink, H. *Acta Crystallogr.* **1991**, *C47*, 1532−1534.

Table 5. Fourier Terms of the ADP Modulation Obtained for the Two Structures

atom	$U_{11} \times \sin(2\pi\bar{x}_4)$	$U_{22} \times \sin(2\pi\bar{x}_4)$	$U_{33} \times \sin(2\pi\bar{x}_4)$	$U_{12} \times \sin(2\pi\bar{x}_4)$	$U_{13} \times \sin(2\pi\bar{x}_4)$	$U_{23} \times \sin(2\pi\bar{x}_4)$	$U_{11} \times \cos(2\pi\bar{x}_4)$	$U_{22} \times \cos(2\pi\bar{x}_4)$	$U_{33} \times \cos(2\pi\bar{x}_4)$	$U_{12} \times \cos(2\pi\bar{x}_4)$	$U_{13} \times \cos(2\pi\bar{x}_4)$	$U_{23} \times \cos(2\pi\bar{x}_4)$
Co(1)	**0**[a]	**0**[a]	**0**[a]	**0**[a]	**0**[a]	**0**[a]	**0**[a]	**0**[a]	**0**[a]	**0**[b]	**0**[a]	**0**[b]
	0[a]	0[a]	0[a]	0[a]	0[a]	0[a]	0[a]	0[a]	0[a]	0[b]	0[a]	0[b]
Al(1)	**0**[a]	**0**[a]	**0**[a]	**0**[a]	**0**[a]	**0**[a]	**0**[a]	**0**[a]	**0**[a]	**0**[b]	**0**[a]	**0**[b]
	0[a]	0[a]	0[a]	0[a]	0[a]	0[a]	0[a]	0[a]	0[a]	0[b]	0[a]	0[b]
Ca	**0**[a]	**0**[a]	**0**[a]	**−0.0006(1)**	**0**[a]	**−0.0008(2)**	**0**[a]	**0**[a]	**0**[a]	**0**[b]	**0**[a]	**0.0014(1)**
	0[a]	0[a]	0[a]	0[b]	0[a]	−0.0007(1)	0[a]	0[a]	0[a]	0[b]	0[a]	0.0016(1)
Co(2)	**0**[b]	**0**[b]	**0**[b]	**0**[b]	**0**[a]	**0**[a]	**−0.0046(7)**	**0**[b]	**0**[b]	**0**[b]	**0**[a]	**0**[a]
	0.0012(3)	0[b]	0[b]	0[b]	0[a]	0[a]	−0.0033(7)	0.0030(8)	0[b]	0[b]	0[a]	0[a]
Al(2)	**0**[b]	**0**[b]	**0**[b]	**0**[b]	**0**[a]	**0**[a]	**−0.0046(7)**	**0**[b]	**0**[b]	**0**[b]	**0**[a]	**0**[a]
	0.0012(3)	0[b]	0[b]	0[b]	0[a]	0[a]	−0.0033(7)	0.0030(8)	0[b]	0[b]	0[a]	0[a]
O(1)	**0**[a]	**0**[a]	**0**[a]	**0**[a]	**0**[b]	**0**[b]	**0**[b]	**0**[b]	**0**[b]	**0**[b]	**0**[a]	**0**[a]
	0[a]	0[a]	0[a]	0[a]	0[b]	0[b]	0[b]	0[b]	0[b]	0[b]	0[a]	0[a]
O(2)	**0**[a]	**0**[a]	**0**[a]	**0**[b]	**0**[a]	**0.0028(7)**	**0**[a]	**0**[a]	**0**[a]	**0**[b]	**0**[a]	**0.0065(7)**
	0[a]	0[a]	0[a]	0[b]	0[a]	0[b]	0[a]	0[a]	0[a]	0[b]	0[a]	0.0065(7)
O(3)	**0**[b]	**0**[b]	**0.009(1)**	**0**[b]	**0**[a]	**0**[a]	**0**[b]	**0**[b]	**0.010(2)**	**0**[b]	**0**[a]	**0**[a]
	0[b]	0[b]	0.005(1)	0[b]	0[a]	0[a]	0.005(1)	0[b]	0.007(2)	0[b]	0[a]	0[a]

[a] Fixed by symmetry. [b] Fixed because not significant within their standard deviations.

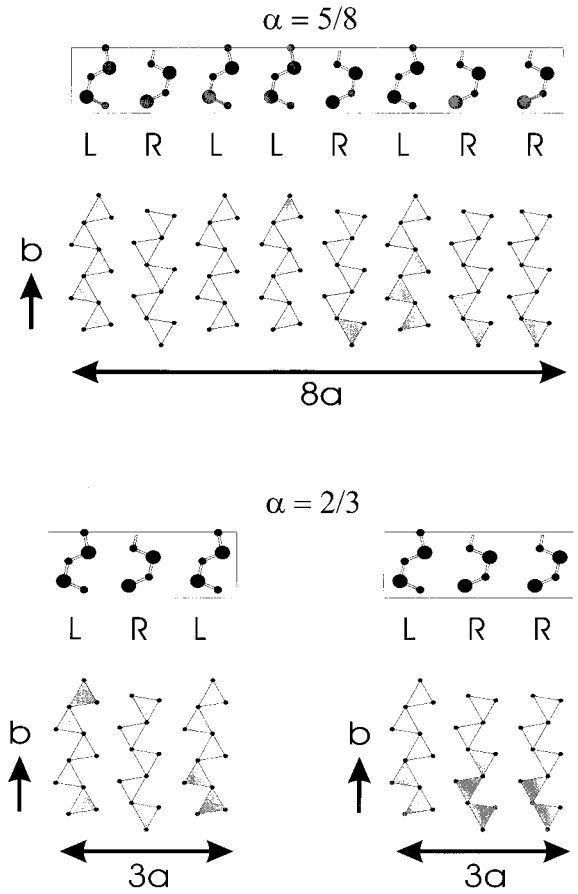

Figure 7. Ordered sequences of the tetrahedral chains along the [100] direction observed for the two studied crystals.

different sites A and B, shown in Figure 6a, vary in a spectacular way versus the *t* parameter (Figure 6b), that is, running along the [100] modulation direction. Two remarkable properties, derived from the refinement results, are to be stressed: First, the A_1 and A_1' sites, related in the average structure by the b glide mirror, exhibit crenel functions centered at the same phase t_0 value, implying a simultaneous occupancy. The same behavior is observed for the B_1 and B_1' sites, symmetry related by this b mirror. Second, the crenel functions of the independent sites A_1, B_1 (and A_1', B_1') are in phase. Indeed, when $\langle X_0 \rangle$ and $\langle x_0 \rangle$ denote the average *x* positions of the A and B sites and X_4^0 and x_4^0 denote the x_4 centering positions of their crenel functions, the relation $X_4^0 - \alpha\langle X_0 \rangle = x_4^0 - \alpha\langle x_0 \rangle$ is verified by the corresponding refined parameters and is not imposed by the 4D symmetry. On the other hand, the crenel function assiociated with the other sites, A_2, A_2', B_2, and B_2', is deduced from the previous one owing to the super glide mirror (^{m}s) which imposes a shift in *t* of $^1/_2$. So, when the sites A_1, A_1', B_1, and B_1' are occupied, the sites A_2, A_2', B_2, and $B_2'$are vacant and vice versa. Last, when the actions of the 4D operators are written on the occupancy functions and the in *t* coincidences of the atom symmetry related by 2_z or b_{0yz} in the average structure are taken into account, two other relations between some independent refinement parameters are verified:

$$X_4^0 - \alpha\langle X_0 \rangle + \alpha/4 \approx +^1/_4$$

$$x_4^0 - \alpha\langle x_0 \rangle + \alpha/4 \approx +^1/_4$$

Note that the last relation is a consequence of the two other ones. As a result of all these observed relations, a perfect order of the two possible configurations $B_1A_1B_1'A_1'$ and $B_2A_2B_2'A_2'$ (Figure 6b) is realized along the [100] modulation direction. So, two types of tetrahedral chains, noted L (left) and R (right-hand), are formed, along [010], corresponding to the configurations $B_1A_1B_1'A_1'$ and $B_2A_2B_2'A_2'$, and can be deduced from each other from the action of pseudoinversion centers. The modulation imposes different sequences of these chains along the [100] direction, depending on the value of the modulation component α (Figure 7). In crystal 2 ($\alpha = {}^2/_3$), a partial disorder is to be excluded, as shown in the previous section (3D symmetry study). However, in this crystal, the two sequences RLR and RLL for the tetrahedral chains appear as equally probable, leading us to assume the existence of domains.

Besides the previous occupancy modulation, modeled with crenel functions, a significant displacive modulation is implied on A, B sites and also on the O(2) and Ca atom positions (Table 4). The shifts of Co(2) and O(3) along [010] from the ideal position in the $m_{(x,0,z)}$ mirror give rise to noticeable displacements (Table 4) for the O(2) and Ca atoms along the same direction.

Let us give some results concerning the bonding scheme. The extremal cation−oxygen distances are

Table 6. Minimum and Maximum Ca−O and Co(1)−O Distances

	d_{min} (Å)	d_{max} (Å)	symmetry code of O atom
Co(1)−O(1)			x, y, z
	1.897(1)	1.936(1)	$-x, 1-y, -z$
	1.901 (1)	**1.932 (1)**	$x, 1-y, z$
			$-x, y, -z$
Co(1)−O(2)	**2.130(1)**	**2.134(1)**	x, y, z
	2.130(1)	2.134(1)	$-x, 1-y, -z$
Ca−O(1)	**2.429(1)**	**2.493(1)**	x, y, z
	2.434(1)	2.492(1)	$x, 1-y, z$
Ca−O(1)	**2.503(1)**	**2.581(1)**	$1-x, 1-y, -z$
	2.503(1)	2.581(1)	$1-x, y, -z$
Ca−O(2)	**2.319(1)**	**2.321(1)**	$1+x, y, z$
	2.315(1)	2.318(1)	
Ca−O(2)	**2.505(2)**	**2.884(2)**	$1/2-x, 1/2-y, z$
	2.509(1)	2.880(1)	$1/2-x, 3/2-y, z$
Ca−O(3)	**2.293(1)**	**2.338(1)**	$1/2-x, 1/2-y, 1/2-z$
	2.314(1)	2.330(1)	$1/2-x, 1/2+y, 1/2-z$

summarized in Table 6. Inside the octahedral layers, the Co(1)−O distances undergo small variations despite the modulation. The distance from the apical O(2) oxygen atom (∼2.13 Å) is much larger than the equatorial distances (∼1.92 Å). These distances are quite similar in the two studied crystals ($\alpha = 5/8$; $2/3$). The same environment is observed for Mn and Al in $Ca_2MnGaO_{5+\delta}$ and Ca_2AlGaO_5 crystals with the brownmillerite type structures.[5,9] The Ca atom exhibits an 8-fold coordination in all the crystal unit cells running along the [100] modulation direction, with distances ranging from 2.30 to 2.90 Å. Only the two Ca−O(2) distances, approximately directed along [010], vary in a large way, as expected (Table 6). Note that the valence of the Ca atom, calculated from the bond valence formalism,[18] keeps a roughly constant value of 2.05 in all the unit cells. Within the tetrahedral layers, the Co(2) and Al(2) atoms show a distorted tetrahedral coordination in all the unit cells, running along the [100] modulation direction. To give a more accurate description of the different environments along [100], the actual Co(2)−O (or Al(2)−O) distances are summarized in Table 7. These distances refer to the tested 3D symmetries *Pcam* ($\alpha = 5/8$) and *Ic*2*m* ($\alpha = 2/3$), corresponding to the 3D symmetry of the supercell. For each tetrahedron, one observes two strong bonds with shorter distances of about 1.75 Å (Table 7) and two relaxed bonds (1.84 Å < d <1.99 Å). As expected, the strong bonds are established with the O(2) apical atoms. From the bond valence formalism,[18] a valence state close to 3.0 is found for Co and Al ($2.95 < s < 3.05$) in each tetrahedron.

A similar coordination (with the same types of cation−oxygen distances) was observed in the $A_2MnGaO_{5+\delta}$ [5,6] (A = Ca, Sr) and Ca_2AlGaO_5 [16] compounds for the Ga atom in the tetrahedral layers. It should be emphasized that the *Ic*2*m* symmetry considered for these crystals (in our axis setting) allows two types of GaO_4 tetrahedral chains to be built in the [010] direction. In contrast, for $(Ca_{1-x}Pr_x)_2(Co_{1-y}Al_y)_2O_5$ crystals,[17] the situation appears to be different. Indeed, within the considered *Pbnm* symmetry, the [(Co, Al)−O_4] tetrahedra are strongly distorted with 1.74 Å (× 2), 1.79 Å, and 2.13 Å distances, but the global character of the [(Co, Al)−O_4] tetrahedral chains is also observed.

Table 7. Co(2)−O Distances in the Two Tetrahedral Layers ($z = 1/4$ and $z = 3/4$), Obtained in the Different Unit Cells for the Two Modulated Studied Crystals

unit cell: n[a]	d(Co(2)−O^{i}(2)) (Å) i: $1/2-x, 1/2-y, z$ i: $1/2-x, 1/2-y, 1/2-z$	d(Co(2)−O^{ii}(3)) (Å) ii: $x, 1-y, z$	d(Co(2)−O^{iii}(3)) (Å) iii: $1/2-x, 1/2-y, 1/2-z$
		Co(2) in (x, y, z)	
$\alpha = 5/8$			
0	1.764(1)	1.846(1)	1.878(1)
1	1.766(1)	1.842(1)	1.880(1)
2	1.762(1)	1.874(1)	1.878(1)
3	1.736(1)	1.883(1)	1.872(1)
4	1.754(1)	1.846(1)	1.878(1)
5	1.766(1)	1.842(1)	1.880(1)
6	1.762(1)	1.874(1)	1.878(1)
7	1.736(1)	1.883(1)	1.872(1)
$\alpha = 2/3$			
0	1.758(1)	1.908(1)	1.851(1)
1	1.759(1)	1.857(1)	1.759(1)
2	1.757(1)	1.873(1)	1.757(1)
unit cell: n[a]	d(Co(2)−O^{i}(2)) (Å) i: $1-x, 1-y, 1/2+z$ i: $1-x, 1-y, 1-z$	d(Co(2)−O^{ii}(3)) (Å) ii: $1/2+x, 1/2-y, 1/2+z$	d(Co(2)−O^{iii}(3)) (Å) iii: $1-x, 1-y, 1-z$
		Co(2) in $(1/2+x, 1/2+y, 1/2+z)$	
$\alpha = 5/8$			
0	1.771(1)	1.886(1)	1.782(1)
1	1.760(1)	1.872(1)	1.857(1)
2	1.729(1)	1.869(1)	1.992(1)
3	1.758(1)	1.884(1)	1.837(1)
4	1.771(1)	1.886(1)	1.782(1)
5	1.760(1)	1.872(1)	1.857(1)
6	1.729(1)	1.869(1)	1.992(1)
7	1.758(1)	1.884(1)	1.837(1)
$\alpha = 2/3$			
0	1.757(1)	1.859(1)	1.894(1)
1	1.759(1)	1.898(1)	1.851(1)
2	1.757(1)	1.894(1)	1.859(1)

[a] The origin of the unit cell is chosen for $n = 0$.

This study shows that the structures of the brownmillerite $Ca_2Co_{2-x}Al_xO_5$ are characterized by a regular alternation of R and L tetrahedral chains. The modulated distribution of these chains can be described by a supercell (the cell parameters j**a**, **b**, **c**), where the SG depends on the parity of the integers i and j, defining the commensurate value ($\alpha = i/j$) of the α component (Table 2). These results suggest that a similar situation could be in fact obtained for the brownmillerites $Ca_2MnGaO_{5+\delta}$ [5] and $Sr_2MnGaO_{5+\delta}$.[6] It is most probable that the structure of theses oxides does not consist of a coexistence of *Ima*2 and *Pnma* domains but results from a modulated distribution of the R and L tetrahedral chains in the structure, the latter being either commensurate or incommensurate. Similarly, the brownmillerite structure of $Ca_2Fe_2O_5$,[1] showing a P lattice with a strong pseudosymmetry character I, can be considered as the limiting case of a modulated structure with a value of the α component equal to 1. Note that the SG symmetry *Pbnm*, referring to our axis setting, is a subgroup of the *Icmm* SG describing the average structure of $Ca_2Co_{2-x}Al_xO_5$. Finally, the *Ic*2*m* SG symmetry, deduced from a limiting value $\langle\langle\alpha = 0\rangle\rangle$, allows a nonmodulated structure to be built, including an unique orientation of tetrahedral chains (either L or R) along the [100] direction.

The origin of the modulated distribution of these two kinds of L and R chains and the influence of the nature of the B cations (electronic configuration, size) and that of the external phenomena (temperature, annealing, quenching) upon the modulation are to date not clear and will require further investigations.

Acknowledgment. The authors are grateful to Mrs. J. Chardon for her technical assistance.

CM011270Z

(18) Brese, N. E.; O'Keefe, M. *Acta Crystallogr.* **1991**, *B47*, 192–197.